Journal of Solid State Chemistry **163,** 121–131 (2002)
doi:10.1006/jssc.2001.9380, available online at http://www.idealibrary.com on IDEAL®

Synthesis and X-Ray Powder Diffraction Study of New Phosphates in the $Cu_3(PO_4)_2$–$Sr_3(PO_4)_2$ System: $Sr_{1.9}Cu_{4.1}(PO_4)_4$, $Sr_3Cu_3(PO_4)_4$, $Sr_2Cu(PO_4)_2$, and $Sr_{9.1}Cu_{1.4}(PO_4)_7$

A. A. Belik, A. P. Malakho, and B. I. Lazoryak[1]

Department of Chemistry, Moscow State University, Moscow 119899, Russia

and

S. S. Khasanov

Institute of Solid State Physics, Chernogolovka 142432, Russia

Received May 29, 2001; in revised form August 21, 2001; accepted August 24, 2001

New phosphates, $Sr_{1.9}Cu_{4.1}(PO_4)_4$, $Sr_2Cu(PO_4)_2$, and $Sr_{9.1}Cu_{1.4}(PO_4)_7$, were found in the $Cu_3(PO_4)_2$–$Sr_3(PO_4)_2$ system at 900°C under air. $Sr_{1.9}Cu_{4.1}(PO_4)_4$ crystallizes in an orthorhombic system with $a = 15.3695(7)$ Å, $b = 10.3652(4)$ Å, and $c = 7.9425(4)$ Å. Crystal structures of $Sr_{9.1}Cu_{1.4}(PO_4)_7$, $Sr_2Cu(PO_4)_2$, and the known phase, $Sr_3Cu_3(PO_4)_4$, were refined by the Rietveld method from X-ray diffraction data: space group $R\bar{3}m$, $a = 10.6119(1)$ Å, $c = 19.7045(2)$ Å, and $Z = 3$ for $Sr_{9.1}Cu_{1.4}(PO_4)_7$; space group $C2/m$, $a = 11.5155(1)$ Å, $b = 5.07543(6)$ Å, $c = 6.57487(7)$ Å, $\beta = 106.3563(6)°$, and $Z = 2$ for $Sr_2Cu(PO_4)_2$; and space group $P2_1/c$, $a = 9.2010(1)$ Å, $b = 4.94104(4)$ Å, $c = 17.8998(3)$ Å, $\beta = 122.8952(9)°$, and $Z = 2$ for $Sr_3Cu_3(PO_4)_4$. A second-harmonic generation study confirmed that the structures of all four compounds have the center of symmetry. $Sr_3Cu_3(PO_4)_4$ is isotypic with $Ca_3Cu_3(PO_4)_4$. Copper cations in $Sr_3Cu_3(PO_4)_4$ have square planar and trigonal bipyramidal coordination and strontium cations have octahedral and ninefold coordination. $Sr_2Cu(PO_4)_2$ is isotypic with $Ba_2Cu(PO_4)_2$. Copper cations in $Sr_2Cu(PO_4)_2$ have square planar coordination and strontium cations have ninefold coordination. $Sr_{9.1}Cu_{1.4}(PO_4)_7$ is structurally related to β-$Ca_3(PO_4)_2$ and $Sr_3(PO_4)_2$. A portion of copper cations in $Sr_{9.1}Cu_{1.4}(PO_4)_7$ fully occupies the trigonal-distorted octahedral site $M5$. The structure of $Sr_{9.1}Cu_{1.4}(PO_4)_7$ has some disordered elements: (1) strontium cations in the $M3$ site statistically occupy four positions near the center of symmetry; (2) orientation disordering of the $P1O_4$ tetrahedra is observed; (3) the $M4$ site is occupied by $0.05Sr^{2+} + 0.2Cu^{2+} + 0.75\square$; and (4) copper cations in the $M4$ site are slightly displaced from the threefold axis with distances between positions about 0.94 Å. Formation of solid solutions $Sr_{9.1-x}Ca_xCu_{1.4}(PO_4)_7$ ($0 \le x \le 9.1$), $Sr_{2-x}Ba_xCu(PO_4)_2$ ($0 \le x \le 2$), and $Sr_{3-x}Ba_xCu_3(PO_4)_4$ ($0 \le x \le 1.5$) was shown.

Key Words: **phosphate; copper; strontium; X-ray diffraction; crystal structure; Rietveld method.**

1. INTRODUCTION

Orthophosphates $M_3(PO_4)_2$ (M^{2+} = Mg, Ca, Zn, Sr, Cd, and Ba) with different substitutions have been extensively studied as luminescence materials (1–5). Binary phosphates of strontium and divalent metals (Mg, Mn, Fe, Co, Ni, Cu, Zn, and Cd) have been studied and characterized by different authors. Crystal structures of α-$SrZn_2(PO_4)_2$ (6), $SrNi_2(PO_4)_2$ (7), $Sr_2Ni(PO_4)_2$ (8), $SrCo_2(PO_4)_2$ (9), $Sr_2Co(PO_4)_2$ (10), $SrMn_2(PO_4)_2$ (11), $Sr_3Cu_3(PO_4)_4$ (12), and $Sr_9Fe_{1.5}(PO_4)_7$ (13) were determined. Phase diagrams $M_3(PO_4)_2$–$Sr_3(PO_4)_2$ were investigated for M = Ca, Mg, Zn (1) and Cd (2). The existence of solid solutions, $Sr_{3-x}Mg_x(PO_4)_2$ ($0.27 \le x \le 1.08$ at 1000°C), $Sr_{3-x}Zn_x(PO_4)_2$ ($0.27 \le x \le 0.81$ at 1025°C), and $Sr_{3-x}Cd_x(PO_4)_2$ ($0.36 \le x \le 0.63$ at 1000°C), isotypic with β-$Sr_3(PO_4)_2$ and compounds, $SrMg_2(PO_4)_2$, β-$SrZn_2(PO_4)_2$, and $SrCd_2(PO_4)_2$, with unknown crystal lattices was found (1, 2). β-$Sr_3(PO_4)_2$ was supposed to be isotypic with β-$Ca_3(PO_4)_2$ (1). The solid solutions $Sr_{3-x}Fe_x(PO_4)_2$ ($0.34 \le x \le 0.43$) with the β-$Sr_3(PO_4)_2$ structure type and the compound $SrFe_2(PO_4)_2$ crystallizing in a monoclinic system were found in the $Fe_3(PO_4)_2$–$Sr_3(PO_4)_2$ system (13). Crystal structures of compounds $M_{3-x}Cu_x(XO_4)_2$ (M = Ca, Sr, Ba; X = P, V, As) usually differ from crystal structures of compounds (similar in stoichiomerty) with other transition metals or magnesium due to the Jahn–Teller distortion

[1] To whom correspondence should be addressed. E-mail: lazoryak@tech.chem.msu.ru.

0022-4596/02 $35.00

caused by copper cations, for example, $BaCu_2(PO_4)_2$ (14) and $BaNi_2(PO_4)_2$ (15), $Ba_2Cu(PO_4)_2$ (16) and $Ba_2Mg(PO_4)_2$ (17), $BaCu_2(VO_4)_2$ (18) and $BaMn_2(VO_4)_2$ (19), and $BaCu_2(AsO_4)_2$ (20) and $BaNi_2(AsO_4)_2$ (21). Copper-containing compounds are interesting because of their magnetic properties.

To our knowledge, in the $Cu_3(PO_4)_2$–$Sr_3(PO_4)_2$ system only one compound, $Sr_3Cu_3(PO_4)_4$, was found (12, 22, 23). $Sr_3Cu_3(PO_4)_4$ was supposed (22) to be isotypic with $Ca_3Cu_3(PO_4)_4$ (24) by a comparison of X-ray powder diffraction patterns. The magnetic properties of the $(Sr_{1-x}Ca_x)_3Cu_3(PO_4)_4$ solid solutions were studied (22, 23). A new form of $Sr_3Cu_3(PO_4)_4$, which is topologically similar but not isotypic with $Ca_3Cu_3(PO_4)_4$, was synthesized by a hydrothermal method and its crystal structure was determined (12). Hereinafter, these two forms of $Sr_3Cu_3(PO_4)_4$ will be denoted as I-$Sr_3Cu_3(PO_4)_4$ and II-$Sr_3Cu_3(PO_4)_4$, respectively.

In this paper, we investigate the $Cu_3(PO_4)_2$–$Sr_3(PO_4)_2$ system at 900°C under air. New phosphates $Sr_{1.9}Cu_{4.1}(PO_4)_4$, $Sr_2Cu(PO_4)_2$, and $Sr_{9.1}Cu_{1.4}(PO_4)_7$ were isolated and the crystal structures of $Sr_{9.1}Cu_{1.4}(PO_4)_7$, $Sr_2Cu(PO_4)_2$, and I-$Sr_3Cu_3(PO_4)_4$ were refined by the Rietveld method.

2. EXPERIMENTAL

Synthesis. Samples in the $Sr_{3-x}Cu_x(PO_4)_2$ system were synthesized from stoichiometric mixtures of CuO (99.9%), $SrCO_3$ (99.999%), and $NH_4H_2PO_4$ (99.999%) by the solid state method. Stoichiometric mixtures were heated very slow up to 600°C and then annealed at 900°C (120 h, ground every 30 h) under air in alumina crucibles. The samples with $x = 0$, 0.289, 0.4, 0.414, 0.429, 1, 1.05, 1.25, 1.5, 1.75, 2, 2.05, 2.075, 2.125, 2.5, and 3 were obtained. After annealing, the samples were quenched at room temperature. For synthesis of solid solutions $Sr_{9.1-x}Ca_xCu_{1.4}(PO_4)_7$ $(0 \le x \le 9.1)$, $Sr_{2-x}Ba_xCu(PO_4)_2$ $(0 \le x \le 2)$, and $Sr_{3-x}Ba_xCu_3(PO_4)_4$ $(0 \le x \le 1.5)$, we used also $CaCO_3$ (99.0%) and $BaCO_3$ (99.0%). Solid solutions $Sr_{9.1-x}Ca_xCu_{1.4}(PO_4)_7$ $(0 \le x \le 9.1)$ were synthesized at 900–920°C followed by quenching in air. Solid solutions $Sr_{2-x}Ba_xCu(PO_4)_2$ $(0 \le x \le 2)$ and $Sr_{3-x}Ba_xCu_3(PO_4)_4$ $(0 \le x \le 1.5)$ were synthesized at 840°C followed by quenching in air.

Make some remarks about the synthesis of the three new compounds in the $Sr_{3-x}Cu_x(PO_4)_2$ system with $x = 0.4$, 1, and 2.05. The single-phased samples $Sr_{1.9}Cu_{4.1}(PO_4)_4$ $(x = 2.05)$ and $Sr_2Cu(PO_4)_2$ $(x = 1)$ could be obtained at 900°C. Annealing of the sample $Sr_{1.9}Cu_{4.1}(PO_4)_4$ at 950°C resulted in the appearance of a liquid phase. This specimen contained I-$Sr_3Cu_3(PO_4)_4$, $Cu_3(PO_4)_2$, and traces of unidentified phases. A long treatment of $Sr_{1.9}Cu_{4.1}(PO_4)_4$ at 950°C resulted in the growth of I-$Sr_3Cu_3(PO_4)_4$ single crystals. Annealing of the blue specimen $Sr_2Cu(PO_4)_2$ at 1020°C resulted in a green powder, which consisted of an unidentified phase (phase I with six strongest lines: $d = 2.657$, 3.121, 2.800, 3.098, 2.784, and 2.702 Å) and traces of $Sr_{9.1}Cu_{1.4}(PO_4)_7$ and I-$Sr_3Cu_3(PO_4)_4$. Traces of phase I, $Sr_{9.1}Cu_{1.4}(PO_4)_7$, and I-$Sr_3Cu_3(PO_4)_4$ appeared when $Sr_2Cu(PO_4)_2$ was annealed at 920°C. Our attempts to synthesize at 900°C the compound $Sr_{9.1}Cu_{1.4}(PO_4)_7$ $(x = 0.4)$ from $SrCO_3$ (99.999%) were not successful, even when platinum crucibles and quenching in liquid nitrogen were used. The specimens in these cases were blue and consisted of three phases, $Sr_3(PO_4)_2$, $Sr_{9.1}Cu_{1.4}(PO_4)_7$, and $Sr_2Cu(PO_4)_2$, in comparable amounts. When the specimen $Sr_{9.1}Cu_{1.4}(PO_4)_7$ was cooled in a furnace, it was light-gray and also consisted of the three phases. The compound $Sr_{9.1}Cu_{1.4}(PO_4)_7$ (with traces of $Sr_3(PO_4)_2$) could be obtained by quenching from 1000°C into air in a platinum crucible. The single-phased sample $Sr_{9.1}Cu_{1.4}(PO_4)_7$ $(x = 0.4)$ in the amount of 0.1 g was obtained in a corundum crucible by quenching from 900°C into air when we used $SrCO_3$ (98.0%), CuO (99.9%), and $NH_4H_2PO_4$ (99.999%) in synthesis. It seems that impurities can stabilize the $Sr_{9.1}Cu_{1.4}(PO_4)_7$ phase.

X-ray diffraction measurements. X-ray powder diffraction (XRD) measurements were performed at room temperature with a SIEMENS D500 Bragg-Brentano-type powder diffractometer equipped with an incident-beam quartz-monochromator to obtain Cu$K\alpha_1$ radiation ($\lambda = 1.5406$ Å) and a BRAUN position-sensitive detector and operated at 30 kV and 30 mA. Silicon was used as an external standard. For phase analysis XRD data were collected in the range $2\theta = 10°$–$60°$ with a step interval of 0.02°. Counting conditions of XRD data collection for crystal structure refinements of $Sr_2Cu(PO_4)_2$, I-$Sr_3Cu_3(PO_4)_4$, and $Sr_{9.1}Cu_{1.4}(PO_4)_7$ are summarized in Table 1. Structure refinements were carried out by the Rietveld method (25) with RIETAN-2000 (26). The split pseudo-Voigt function of Toraya (27) was fit to each profile, and the ninth-order Legendre polynomials to the background. Partial profile relaxation (26) was applied to 012, 110, 015, 122, 205, 220, 404, 045, and 324 reflections for $Sr_{9.1}Cu_{1.4}(PO_4)_7$, 001, 110, -111, -202, 002, 310, 020, 022, and -222 reflections for $Sr_2Cu(PO_4)_2$, and 100, 011, -202, -213, -115, and 202 reflections for I-$Sr_3Cu_3(PO_4)_4$ to improve fits in these reflections at the last stages of the structure refinements. Preferred orientation was corrected with the March–Dollase function on the assumption of the (001) preferred orientation vector for $Sr_2Cu(PO_4)_2$ and (010) for I-$Sr_3Cu_3(PO_4)_4$. Atomic scattering factors for Sr^{2+}, Cu^{2+}, P, and O^- were taken from (28). Standard deviations were estimated by the conventional method.

Second-harmonic generation (SHG) study. The second-harmonic generation response of powder samples was measured in the reflection scheme. A Q-switch pulsed Nd:YAG

TABLE 1
Conditions of the Diffraction Experiments and Parts of Refinement Results for I-$Sr_3Cu_3(PO_4)_4$, $Sr_2Cu(PO_4)_2$, and $Sr_{9.1}Cu_{1.4}(PO_4)_7$

	I-$Sr_3Cu_3(PO_4)_4$	$Sr_2Cu(PO_4)_2$	$Sr_{9.1}Cu_{1.4}(PO_4)_7$
Space group	$P2_1/c$ (No. 14)	$C2/m$ (No. 12)	$R\bar{3}m$ (No. 166)
Z	2	2	3
2θ range (°)	10–140	7–100	10–110
Scan step (°)	0.02	0.02	0.02
I_{max} (counts)	55429	87889	87791
Lattice constants:			
a (Å)	9.2010(1)	11.5155(1)	10.6119(1)
b (Å)	4.94104(4)	5.07543(6)	
c (Å)	17.8998(3)	6.57487(7)	19.7045(2)
β (°)	122.8952(9)	106.3563(6)	
V (Å^3)	683.30(2)	368.724(7)	1921.69(3)
Number of Bragg reflections	1290	217	330
Variables:			
Structure/lattice	48/4	17/4	32/2
Background/profile	10/10	10/10	10/10
Scale/shifts/texture	1/2/1	1/2/1	1/2/—
PPP[a]	25	35	35
Texture parameter	1.0253(10)	0.9308(9)	—
R_{wp}, R_p	5.01%; 3.80%	4.67%; 3.35%	5.16%; 3.94%
R_B; R_F	1.75%; 0.65%	1.98%; 1.10%	3.81%; 1.98%
S	1.97	2.47	2.07
R_{wp}*, R_p*	6.56%; 4.67%	5.56%; 3.98%	6.04%; 4.61%
R_B*, R_F*	1.71%; 0.66%	1.92%; 1.14%	3.77%; 1.93%
S*	2.57	2.93	2.41

[a] Refined primary profile parameters (PPP). R factors without stars are after applying partial profile relaxation and with stars before applying partial profile relaxation.

laser operating at $\lambda_\omega = 1064$ nm was used as the radiation source with a repetition rate of 4 impulses/s and a duration of impulses of about 12 ns. The laser beam was split into two beams to excite the radiation at doubled frequency ($\lambda_{2\omega} = 532$ nm) simultaneously in samples under investigation and in a reference sample. The incident beam peak power was about 0.1 MW on a spot of 3-mm diameter on the surface of the sample. Powdered crystalline α-SiO_2 was used as a reference sample.

3. RESULTS AND DISCUSSION

Phase Analysis

The single-phased samples were obtained for $x = 0$, 0.4, 1, 1.5, 2.05, and 3. All other samples were two-phased and contained the neighboring single-phased compounds. The single-phased samples had the following colors: white for $x = 0$, light-blue for $x = 0.4$, deep blue for $x = 1$, gray-blue for $x = 1.5$, and malachite-green for $x = 2.05$ and 3. Thus, four binary compounds are formed at 900°C in the $Sr_{3-x}Cu_x(PO_4)_2$ system: $Sr_{1.9}Cu_{4.1}(PO_4)_4$, I-$Sr_3Cu_3(PO_4)_4$, $Sr_2Cu(PO_4)_2$, and $Sr_{9.1}Cu_{1.4}(PO_4)_7$.

XRD patterns of $Sr_{1.9}Cu_{4.1}(PO_4)_4$ and $Sr_2Cu(PO_4)_2$ were indexed with the TREOR90 program (29). $Sr_{1.9}Cu_{4.1}(PO_4)_4$ was indexed in an orthorhombic system with $a = 15.3695(7)$ Å, $b = 10.3652(4)$ Å, and $c = 7.9425(4)$ Å ($M_{20} = 32.5$, $F_{30} = 68.6$ (0.0073, 60), indexing was made using 122 reflections in the range $2\theta = 10°$–$62°$). Figure 1a shows a portion of the XRD pattern for $Sr_{1.9}Cu_{4.1}(PO_4)_4$. The XRD pattern of $Sr_2Cu(PO_4)_2$ was indexed in a C-centered monoclinic cell with $a = 11.5155(4)$ Å, $b = 5.0753(2)$ Å, $c = 6.5747(2)$ Å, and $\beta = 106.357(3)°$ ($M_{20} = 58.2$, $F_{30} = 75.9$ (0.0092, 43), indexing was made using 123 reflections in the range $2\theta = 10°$–$90°$). The unit cell parameters of $Sr_2Cu(PO_4)_2$ was found to be similar with $Ba_2Cu(PO_4)_2$ (16): $a = 12.160$ Å, $b = 5.133$ Å, $c = 6.885$ Å, $\beta = 105.42°$, and space group $C2/m$. But we could not find any isostructural compounds among $AM_2(XO_4)_2$ (A = Ca, Sr, Ba; M = Mg, Mn, Co, Ni, Cu, Zn; X = P, V, As) for $Sr_{1.9}Cu_{4.1}(PO_4)_4$. With crystal structure information for $Sr_9Fe_{1.5}(PO_4)_7$ (13) and $Ca_3Cu_3(PO_4)_4$ (24), indexing of XRD patterns for $Sr_{9.1}Cu_{1.4}(PO_4)_7$ and I-$Sr_3Cu_3(PO_4)_4$ was carried out in a trigonal system with unit cell parameters $a = 10.6104(2)$ Å and $c = 19.7013(5)$ Å ($M_{20} = 264.5$, $F_{30} = 169.4$ (0.0049, 36), indexing was made using 118 reflections in the range $2\theta = 10°$–$81°$), and in a primitive monoclinic cell with unit cell parameters $a = 9.2018(6)$ Å, $b = 4.9414(3)$ Å, $c = 17.903(1)$ Å, and $\beta = 122.895(5)°$ ($M_{20} = 55.7$, $F_{30} = 114.3$ (0.0060, 44), indexing was made using 107 reflections in the range $2\theta = 10°$–$60°$), respectively. Index results for $Sr_{1.9}Cu_{4.1}(PO_4)_4$, I-$Sr_3Cu_3(PO_4)_4$, $Sr_2Cu(PO_4)_2$, and $Sr_{9.1}Cu_{1.4}(PO_4)_7$ will be published in the Powder Diffraction File. All four compounds (with $x = 0.4$, 1, 1.5, and 2.05) showed no SHG response. These data confirmed that crystal structures of $Sr_2Cu(PO_4)_2$ and I-$Sr_3Cu_3(PO_4)_4$ have the center of symmetry as for isotypic compounds, $Ba_2Cu(PO_4)_2$ (space group $C2/m$) (16) and $Ca_3Cu_3(PO_4)_4$ (space group $P2_1/c$) (24), respectively. SHG data also indicated that crystal structures of $Sr_{1.9}Cu_{4.1}(PO_4)_4$ and $Sr_{9.1}Cu_{1.4}(PO_4)_7$ have the center of symmetry.

Structure Refinements

The crystal structure refinement of I-$Sr_3Cu_3(PO_4)_4$ with the initial atomic coordinates for II-$Sr_3Cu_3(PO_4)_4$ ($a = 18.439$ Å, $b = 4.921$ Å, $c = 18.035$ Å, and $\beta = 123.25°$ in space group $A2/n$) (12) resulted in a part of weak reflections not being fitted, while all strong reflections were fitted rather well. In addition, the calculated XRD pattern contained some weak reflections, which were absent on the observed XRD pattern. When atomic coordinates for $Ca_3Cu_3(PO_4)_4$ ($a = 8.917$ Å, $b = 4.8995$ Å, $c = 17.619$ Å, and $\beta = 124.08°$ in space group $P2_1/c$) (24) were used as the starting model, all reflections were fitted. The refinement of the crystal structure of I-$Sr_3Cu_3(PO_4)_4$ in the latter model converged

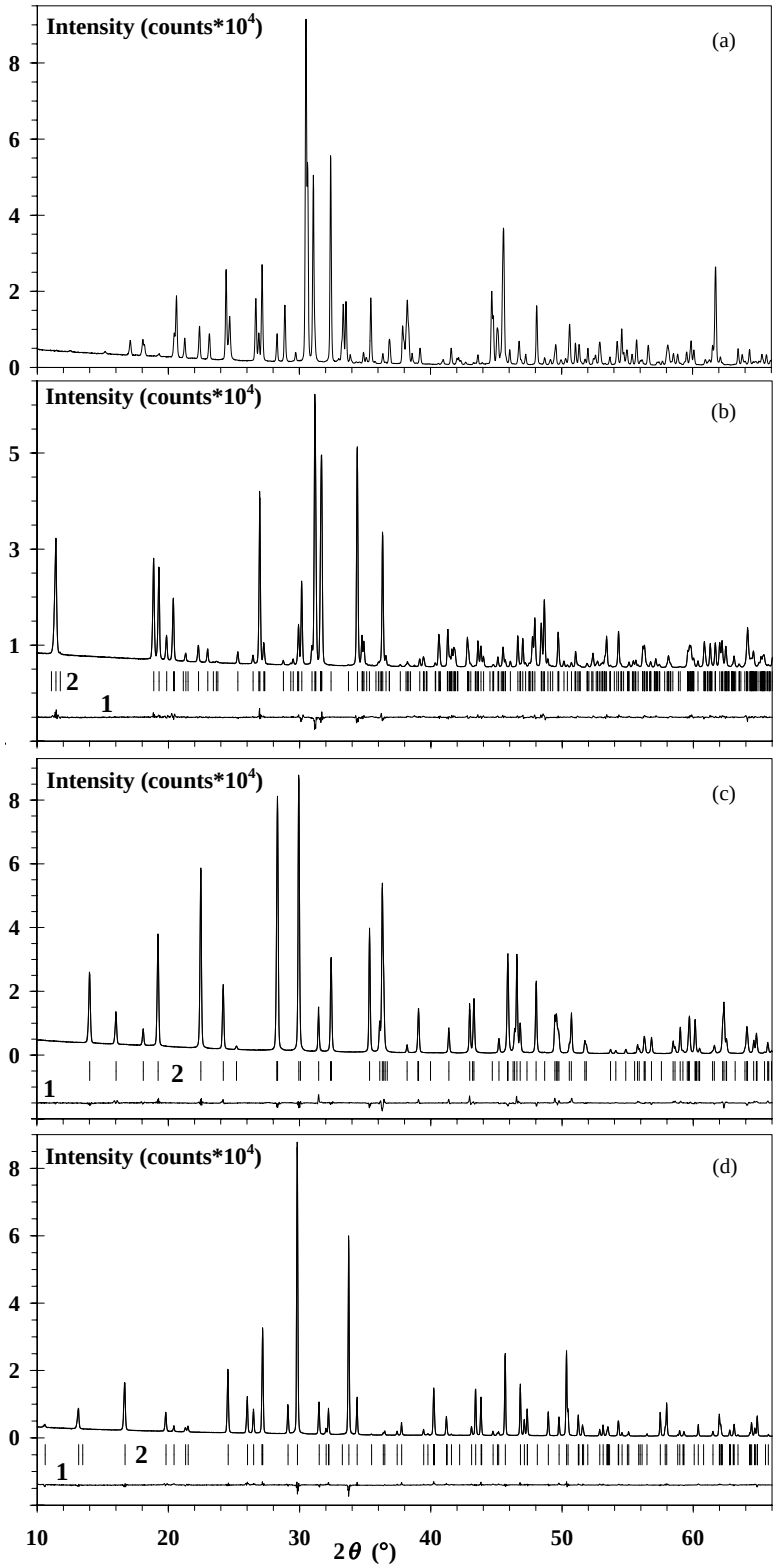

FIG. 1. Portions of XRD patterns and Rietveld refinement profiles for (a) $Sr_{1.9}Cu_{4.1}(PO_4)_4$, (b) I-$Sr_3Cu_3(PO_4)_4$, (c) $Sr_2Cu(PO_4)_2$, and (d) $Sr_{9.1}Cu_{1.4}(PO_4)_7$. 1, difference XRD patterns; 2, Bragg reflections.

TABLE 2
Fractional Coordinates and Atomic Displacement Parameters for I-$Sr_3Cu_3(PO_4)_4$

Atom	*x*	*y*	*z*	*B* (Å^2)
Cu1	0	0	0	0.55(3)
Cu2	0.94707(14)	0.4682(3)	0.12149(7)	0.64(3)
Sr1	0.5	0	0.5	0.94(3)
Sr2	0.71968(9)	0.4649(2)	0.26364(5)	0.43(2)
P1	0.2346(3)	−0.0105(5)	0.58723(13)	0.39(4)
P2	0.2061(3)	0.0228(5)	0.83698(13)	0.53(5)
O1	0.4110(7)	−0.0881(11)	0.6718(3)	0.98(12)
O2	0.2368(6)	0.5570(11)	0.0032(3)	0.5*
O3	0.1836(6)	0.2879(10)	0.5932(3)	0.5*
O4	0.0896(6)	−0.1981(9)	0.5827(3)	0.06(11)
O5	0.3759(6)	−0.1355(9)	0.8924(3)	0.53(11)
O6	0.0614(6)	−0.0773(10)	0.8519(3)	0.54(11)
O7	0.2371(6)	0.1640(9)	0.3568(3)	0.09(11)
O8	0.1473(5)	−0.0178(12)	0.7377(3)	0.11(10)

*Fixed values. All sites have the occupancy equal to 1.

successfully and good agreement between the observed and calculated XRD patterns was obtained (Fig. 1b). Table 1 presents the final *R* factors and lattice parameters. Final fractional coordinates and atomic displacement parameters for I-$Sr_3Cu_3(PO_4)_4$ are listed in Table 2 and metal–oxygen bond lengths and angles in Table 3.

The crystal structure refinement of $Sr_2Cu(PO_4)_2$ using the atomic coordinates of $Ba_2Cu(PO_4)_2$ (16) as the starting

TABLE 3
Bond Distances (Å) and Angles (°) for Tetrahedra PO_4^{3-} in I-$Sr_3Cu_3(PO_4)_4$

Bonds and angles		Bonds and angles	
Cu1–O3 (×2)	1.917(5)	Sr2–O1	2.463(5)
–O4 (×2)	1.942(5)	–O3	2.524(5)
Cu2–O8	1.902(4)	–O8	2.532(6)
–O2	1.939(5)	–O7	2.590(4)
–O6	2.001(5)	–O4	2.672(5)
–O4	2.117(5)	–O6	2.701(5)
–O7	2.162(5)	–O1a	2.786(5)
–O3	2.791(5)	–O5	2.925(5)
Sr1–O5 (×2)	2.423(5)	–O8a	2.999(6)
–O2 (×2)	2.469(4)		
–O7 (×2)	2.519(5)		
P1–O2	1.532(5)	P2–O5	1.534(5)
–O1	1.550(6)	–O8	1.565(4)
–O3	1.569(5)	–O6	1.573(4)
–O4	1.590(5)	–O7	1.579(5)
O1–P1–O2	110.9(3)	O5–P2–O6	112.9(3)
O1–P1–O3	111.0(3)	O5–P2–O7	111.0(3)
O1–P1–O4	108.1(3)	O5–P2–O8	105.7(3)
O2–P1–O3	111.9(3)	O6–P2–O7	109.7(3)
O2–P1–O4	108.7(3)	O6–P2–O8	110.5(3)
O3–P1–O4	106.1(3)	O7–P2–O8	106.8(3)

TABLE 4
Fractional Coordinates and Atomic Displacement Parameters for $Sr_2Cu(PO_4)_2$

Atom	*x*	*y*	*z*	*B* (Å^2)
Cu	0	0.5	0.5	0.48(3)
Sr	0.17120(5)	0	0.21669(8)	0.40(2)
P	0.14221(13)	0	0.7099(2)	0.42(3)
O1	0.0499(3)	0	0.8346(5)	0.68(8)
O2	0.2711(3)	0	0.8628(4)	0.29(7)
O3	0.1295(2)	0.2463(4)	0.5606(3)	0.55(6)

Note. All sites have the occupancy equal to 1.

model converged successfully. Reasonable atomic displacement parameters and interatomic distances were obtained (Tables 4 and 5). Table 1 gives *R* factors and lattice parameters. Figure 1c displays a portion of the observed, calculated, and difference XRD patterns for $Sr_2Cu(PO_4)_2$.

The structural data of $Ca_9Cu_{1.5}(PO_4)_7$ (30) were used as an initial model for the structure refinement of $Sr_{9.1}Cu_{1.4}(PO_4)_7$. $Ca_9Cu_{1.5}(PO_4)_7$ (space group *R*3*c*, $a = 10.3379$ Å, $c = 37.1898$ Å, and $Z = 6$) is isotypic with β-$Ca_3(PO_4)_2$ (31) and has six cation sites *M*1–*M*6 (32). The following cation distribution was used as an initial cation distribution for $Sr_{9.1}Cu_{1.4}(PO_4)_7$: $1Sr^{2+}$ in *M*1, $1Sr^{2+}$ in *M*2, $1Sr^{2+}$ in *M*3, $0.4Cu^{2+} + 0.1Sr^{2+} + 0.5\square$ in *M*4, $1Cu^{2+}$ in *M*5, and $1\square$ in *M*6 ($\square$, vacancy). The occupancy of the *M*4 site was deduced from the total composition of the sample. The refinement in this model gave good agreement between the observed and calculated XRD patterns ($R_{wp} = 7.19\%$ ($S = 2.84$), $R_p = 5.31\%$, $R_B = 3.94\%$, and $R_F = 2.47\%$). But difficulties appeared in the localization of oxygen atoms around the P1 position; it was also discovered that some cations occupied the *M*6 site, and some oxygen atoms had negative atomic displacement parameters in the *R*3*c* model. A rather satisfactory description of the crystal structure of $Sr_{9.1}Cu_{1.4}(PO_4)_7$ in the *R*3*c* model indicates that the structures of $Sr_{9.1}Cu_{1.4}(PO_4)_7$ and $Ca_9Cu_{1.5}(PO_4)_7$ do not significantly differ from each other.

TABLE 5
Bond Distances (Å) and Angles (°) for Tetrahedra PO_4^{3-} in $Sr_2Cu(PO_4)_2$

Bonds		Bonds and angles	
Sr–O1	2.473(3)	P–O1	1.514(3)
–O1a	2.507(3)	–O2	1.540(3)
–O3 (×2)	2.679(2)	–O3 (×2)	1.571(2)
–O2 (×2)	2.711(1)	O1–P1–O2	109.9(2)
–O3a (×2)	2.742(2)	O1–P1–O3 (×2)	112.49(13)
–O2a	2.871(3)	O2–P1–O3 (×2)	108.12(11)
Cu–O3 (×4)	1.925(2)	O3–P1–O3a	105.5(2)

TABLE 6
Fractional Coordinates and Atomic Displacement Parameters for $Sr_{9.1}Cu_{1.4}(PO_4)_7$

Atom[a]	Site	n	x	y	z	B (Å^2)
$M1$	18h	1	0.19082(4)	0.80918	0.53685(3)	0.74(2)
$M31$	18h	$\frac{1}{4}$	0.4920(3)	0.5080	0.0069(4)	0.39(5)[b]
$M32$	18h	$\frac{1}{4}$	0.4682(2)	0.5318	0.0135(2)	0.39[b]
$M41$	6c	$\frac{1}{20}$	0	0	0.363(4)	4.7[c]
$M42$	18h	$\frac{1}{15}$	0.0295(12)	0.9705	0.360(2)	4.7(5)[c]
$M5$	3a	1	0.0	0.0	0.0	0.78(5)
P1	3b	1	0.0	0.0	0.5	3.06(14)
P2	18h	1	0.49238(9)	0.50762	0.39690(11)	1.07(4)
O11	36i	$\frac{1}{3}$	0.9046(14)	0.0431(14)	0.5381(4)	5.4(4)
O21	18h	1	0.5365(2)	0.4635	0.6781(2)	1.42(10)
O22	36i	1	0.2642(3)	0.0104(2)	0.23416(14)	0.47(6)
O24	18h	1	0.9128(2)	0.0872	0.0669(2)	0.81(9)

[a] The $M1$, $M31$, $M32$, and $M41$ sites are occupied by Sr^{2+}; the $M42$ and $M5$ sites are occupied by Cu^{2+}.
[b] Constrained values.
[c] Constrained values.

As our SHG study showed, the structure of $Sr_{9.1}Cu_{1.4}(PO_4)_7$ has a center of symmetry, while the structure of $Ca_9Cu_{1.5}(PO_4)_7$ does not have a center of symmetry (30). Moreover, examination of the *hkl* list for the observed reflections in the $R3c$ model of the crystal structure of $Sr_{9.1}Cu_{1.4}(PO_4)_7$ revealed that all l indexes were even. These facts allowed us to reduce the c parameter by a factor of 2 and to transform the atomic coordinates from space group $R3c$ to $R\bar{3}m$ (as $R3c \rightarrow R\bar{3}c \rightarrow R\bar{3}m$) according to the cell transformation $\mathbf{a}' = -\mathbf{a}, \mathbf{b}' = -\mathbf{b}, 2\mathbf{c}' = \mathbf{c}$. This procedure was described in more details for the crystal structure refinement of $Sr_9Fe_{1.5}(PO_4)_7$ (13). In the $R\bar{3}m$ model, the $M1$ and $M2$, $M4$ and $M6$ sites, and the $P2O_4$ and $P3O_4$ tetrahedra of the $Ca_9Cu_{1.5}(PO_4)_7$ structure are equivalent. The P1, $M3$, and $M5$ sites lie in centers of symmetry (sites 3b, 9e, and 3a, respectively). Hereafter, for the structure of $Sr_{9.1}Cu_{1.4}(PO_4)_7$ we retained the same site numeration as for $Ca_9Cu_{1.5}(PO_4)_7$ (30) and other compounds isotypic with β-$Ca_3(PO_4)_2$ (32–35). The following cation distribution was assumed as an initial cation distribution in the $R\bar{3}m$ model: $1Sr^{2+}$ in $M1$, $1Sr^{2+}$ in $M3$, $0.2Cu^{2+} + 0.05Sr^{2+} + 0.75\square$ in $M4$, and $1Cu^{2+}$ in $M5$.

Further refinement in the $R\bar{3}m$ model showed that strontium cations in the $M3$ site had $B = 6.6(2)$ and cations in the $M4$ site had $B = 10.0(4)$. The displacement of strontium cations in the $M3$ site from site 9e in the center of symmetry $(\frac{1}{2}, \frac{1}{2}, 0)$ to the half-occupied 18h site $(x, -x, z)$ gave $B = 1.4(1)$. The crystal structure refinement of $Sr_{9.2}Co_{1.3}(PO_4)_7$ (36) from single-crystal data showed that in reality strontium cations in the $M3$ sites are disordered over four positions. Additional splitting of strontium cations in the $M3$ sites in the structure of $Sr_{9.1}Cu_{1.4}(PO_4)_7$ over two 18h sites, $M31$ and $M32$, with $n = \frac{1}{4}$ (where n is occupancy) was successful and led to common $B = 0.39(5)$. Note that the refinement of strontium cations in two 18h sites, $M31$ and $M32$, resulted in the lower R factors ($R_{wp} = 5.16\%$ ($S = 2.07$), $R_p = 3.94\%$, $R_B = 3.81\%$, and $R_F = 1.98\%$) in comparison with the refinement in one 18h site, $M3$ ($R_{wp} = 5.73\%$ ($S = 2.30$), $R_p = 4.26\%$, $R_B = 3.98\%$, and $R_F = 2.11\%$). The displacement of cations $(0.8Cu^{2+} + 0.2Sr^{2+})$ in the $M4$ site from site 6c $(0, 0, z)$ with $n = \frac{1}{4}$ to site 18h $(x, -x, z)$ with $n = \frac{1}{12}$ gave $B = 3.2(4)$. But this led to short distances $M4$–O11 (2.14 Å) and $M4$–O21 (2.21 Å) for strontium cations. Thus, copper and strontium

TABLE 7
Bond Distances (Å) and Angles (°) for Tetrahedra PO_4^{3-} in $Sr_{9.1}Cu_{1.4}(PO_4)_7$

Bonds		Bonds and angles	
$M1$–O22 (×2)	2.536(3)	$M31$–O22 (×2)	2.490(7)
–O24 (×2)	2.602(2)	–O21 (×2)	2.694(4)
–O22a (×2)	2.651(2)	–O22a (×2)	2.614(7)
–O21	2.585(4)	–O21a (×2)	2.913(4)
–O11 (×2)	2.694(8)	–O11 (×2)	2.920(9)
–O11a (×2)	2.80(2)	$M31$–$M31a$[a]	0.401(8)
$M41$–O21 (×3)	2.419(14)	$M31$–$M32$[a]	0.456(7)
–O11 (×6)	2.35(7)	$M31$–$M32a$[a]	0.835(3)
$M41$–$M42$[a]	0.55(3)		
$M32$–O21 (×2)	2.438(3)	$M42$–O21 (×2)	2.193(10)
–O11 (×2)	2.583(8)	–O21a	2.95(2)
–O22 (×2)	2.588(5)	–O11 (×2)	2.16(4)
–O22a (×2)	2.660(4)	–O11a	2.55(3)
$M32$–$M32a$[a]	1.124(7)	–O11b	2.65(3)
		$M42$–$M42a$[a]	0.94(4)
$M5$–O24 (×6)	2.075(3)	O24–Cu5–O24a	96.0(2)
P1–O11 (×12)	1.503(6)	O21–P2–O22 (×2)	108.5(2)
P2–O21	1.571(4)	O21–P2–O24	112.1(2)
–O22 (×2)	1.551(3)	O22–P2–O22a	112.8(2)
–O24	1.602(3)	O22–P2–O24 (×2)	107.5(2)

[a] Distances between split positions. Distances for all split positions O11 are given.

TABLE 8
Unit Cell Parameters in Solid Solutions $Sr_{2-x}Ba_xCu(PO_4)_2$ (I), $Sr_{3-x}Ba_xCu_3(PO_4)_4$ (II), and $Sr_{9.1-x}Ca_xCu_{1.4}(PO_4)_7$ (III)

Composition	a (Å)	b (Å)	c (Å)	β (°)
I, $x = 0.5$	11.816(1)	5.0980(4)	6.7404(6)	105.801(6)
II, $x = 1.5$	9.3484(7)	4.9974(3)	18.007(2)	122.21(1)
III, $x = 9.1$	10.3399(3)		37.1967(7)	
III, $x = 6.825$	10.4357(3)		37.3701(7)	
III, $x = 4.55$	10.5053(3)		19.1887(4)	
III, $x = 2.1$	10.5700(3)		19.4984(4)	
III, $x = 0.7$	10.6055(3)		19.6613(4)	

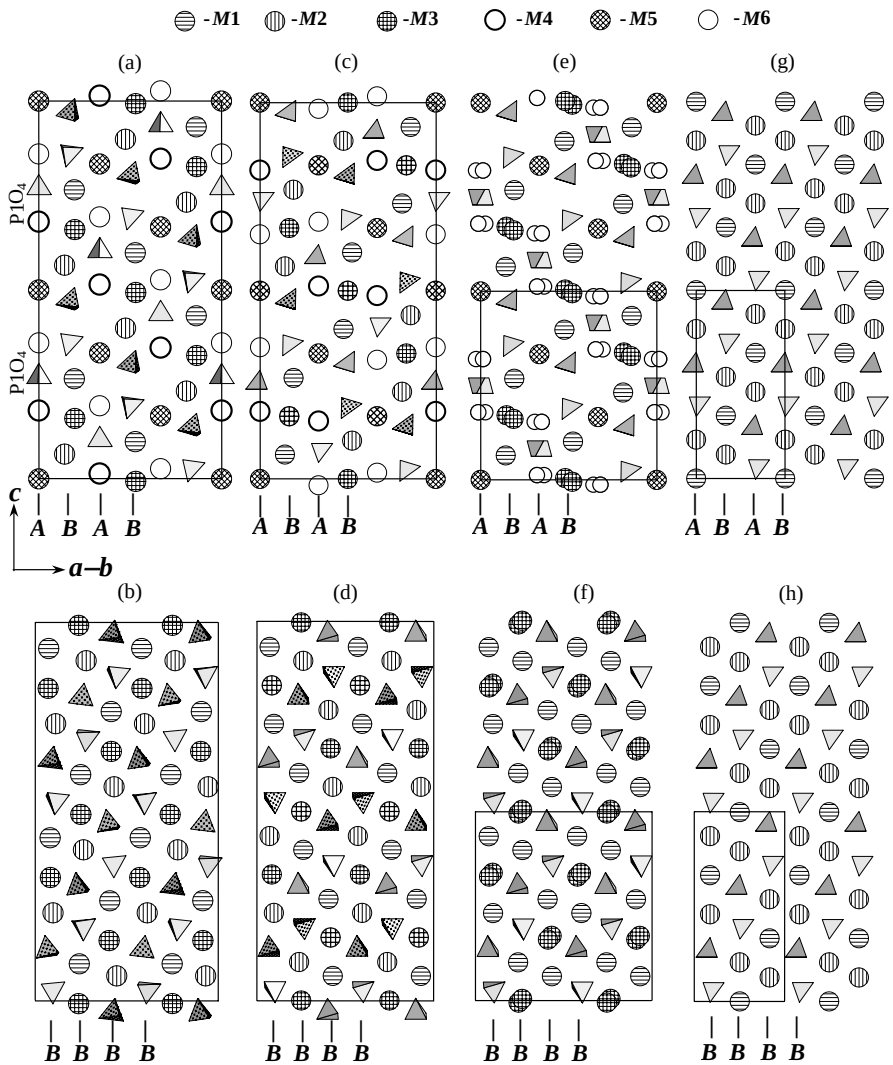

FIG. 2. Projections of crystal structures of (a, b) β-$Ca_3(PO_4)_2$ (space group $R3c$), (c, d) ideal centrosymmetric β-$Ca_3(PO_4)_2$-like structure (space group $R\bar{3}$), (e, f) $Sr_{9.1}Cu_{1.4}(PO_4)_7$ (space group $R\bar{3}m$), and (g, h) $Sr_3(PO_4)_2$ (space group $R\bar{3}m$) viewed along the [110] direction. Columns A and B are marked. Layers I (b, d, f, h) and layers II (a, c, e, g) and unit cells are shown. The disordered $P1O_4$ tetrahedra and split sites $M3$ and $M4$ are shown for the structure of $Sr_{9.1}Cu_{1.4}(PO_4)_7$ (e, f).

cations in the $M4$ site were split: strontium cations were retained in site 6c $(0, 0, z)$ with $n = \frac{1}{20}$ ($M41$), while copper cations were displaced from the threefold axis to site 18h $(x, -x, z)$ with $n = \frac{1}{15}$ ($M42$). Note that occupancies for copper and strontium cations in the $M4$ sites were fixed from the total composition of the sample and were not refined. Splitting of copper cations in the $M4$ sites was also found in the structurally related compound $Ca_9Cu_{1.5}(PO_4)_7$ (30). Tetrahedron $P2O_4$ was localized quite easily, while difficulties appeared in the localization of oxygen atoms around the P1 position. Thermal parameters for oxygen atoms O11 (site 6c) and O12 (site 18h) were large: $B = 68(9)$ and $B = 4.5(4)$, respectively. We examined different models of oxygen surrounding the P1 site. The best model for X-ray powder diffraction data was obtained when oxygen atoms O11 and O12 in the half-occupied special positions 6c (0, 0, z) and 18h $(x, -x, z)$ (the initial model) were refined as one oxygen atom O11 in a general position 36i (x, y, z) with $n = \frac{1}{3}$. The $R\bar{3}m$ model led to the increased atomic displacement parameters for the P1 ($B = 3.06(14)$) and O11 ($B = 5.4(4)$) atoms that may be caused by the disordered character of the $P1O_4$ tetrahedron. Note that the refined occupancy for the O11 site was close to $\frac{1}{3}$ ($n = 0.332(3)$) when B was fixed at the value 3.0.

We also tried to use the atomic coordinates of $Sr_3(PO_4)_2$ (37) (transformed according to $\mathbf{a}' = -2\mathbf{a}$, $\mathbf{b}' = -2\mathbf{b}$, $\mathbf{c}' = \mathbf{c}$) as an initial model. But the refinement was not successful until columns A in the structure of $Sr_3(PO_4)_2$ were modified in that way as they are in the structure of β-$Ca_3(PO_4)_2$ (see Structure Description Section).

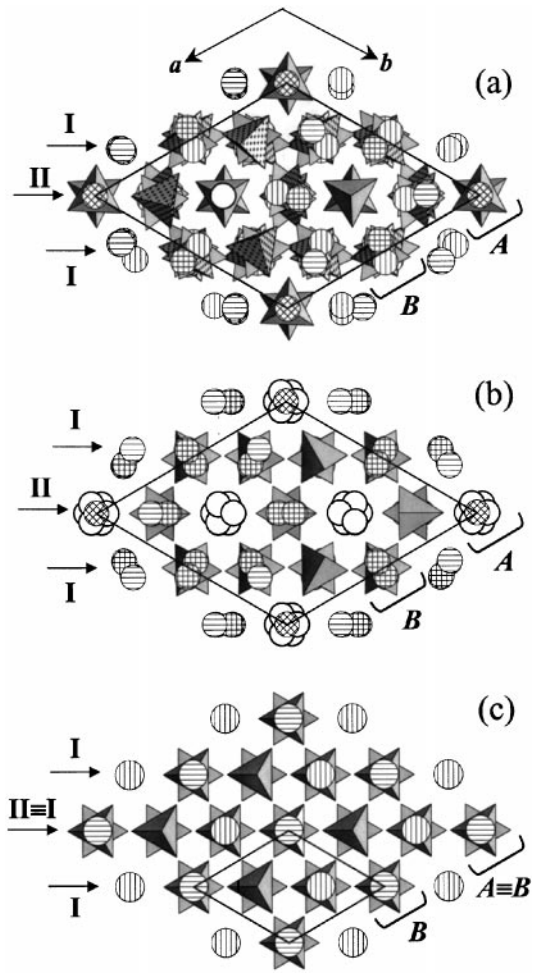

FIG. 3. Projections of crystal structures of (a) β-$Ca_3(PO_4)_2$, (b) $Sr_{9.1}Cu_{1.4}(PO_4)_7$, and (c) $Sr_3(PO_4)_2$ viewed along the [001] direction. Layers I and II and columns *A* and *B* are marked. Unit cells are shown. The split sites *M*3 and *M*4 are shown for the structure of $Sr_{9.1}Cu_{1.4}(PO_4)_7$ (disordered $P1O_4$ tetrahedra are not shown). Atom labels are the same as those in Fig. 2.

Table 1 lists *R* factors and lattice parameters for $Sr_{9.1}Cu_{1.4}(PO_4)_7$. Final fractional coordinates and atomic displacement parameters are listed in Table 6 and metal–oxygen bond lengths and angles in Table 7. Figure 1d displays a portion of the observed, calculated, and difference XRD patterns for $Sr_{9.1}Cu_{1.4}(PO_4)_7$.

Structure Descriptions and Relationships

I-$Sr_3Cu_3(PO_4)_4$ obtained by the solid state method is isotypic with $Ca_3Cu_3(PO_4)_4$ (24) and $Ca_3Cu_3(AsO_4)_4$ (38) in comparison with II-$Sr_3Cu_3(PO_4)_4$ obtained by the hydrothermal method (12). Copper cations in I-$Sr_3Cu_3(PO_4)_4$ occupy two positions: one has square planar coordination and another has trigonal bipyramidal coordination. Strontium cations occupy two positions with octahedral and ninefold coordination. Dimensions of the polyhedra $Sr1O_6$ ($Ca1O_6$) and $Sr2O_9$ ($Ca2O_9$) in I-$Sr_3Cu_3(PO_4)_4$ and $Ca_3Cu_3(PO_4)_4$ are adopted to sizes of cations located in these positions. The size of the $Sr2O_9$ polyhedron may likely be adopted to barium cations. To examine this suggestion, we studied the formation of solid solutions $Sr_{3-x}Ba_xCu_3(PO_4)_4$. It was shown that these solid solutions are formed for $0 \le x \le 1.5$ at 840°C (Table 8), which corresponds to the partial (75%) occupation of the nine-coordinated site by barium cations. In samples with $x > 1.5$ impurity phases were detected.

Copper cations in $Sr_2Cu(PO_4)_2$ have square planar coordination and strontium cations have ninefold coordination. $Sr_2Cu(PO_4)_2$ is more stable than $Ba_2Cu(PO_4)_2$ (also blue in color) (16). The latter compound decomposes above 795–810°C, also giving a green product (16). But our attempts to synthesize $Ca_2Cu(PO_4)_2$ at 900°C were not successful. The formation of solid solutions $Sr_{2-x}Ba_xCu(PO_4)_2$ ($0 \le x \le 2$) was confirmed (Table 8), as might be expected from the isotypic crystal structures of $Sr_2Cu(PO_4)_2$ and $Ba_2Cu(PO_4)_2$.

The structure of $Sr_{9.1}Cu_{1.4}(PO_4)_7$ is related to β-$Ca_3(PO_4)_2$ (31) and $Sr_3(PO_4)_2$ (space group $R\bar{3}m$,

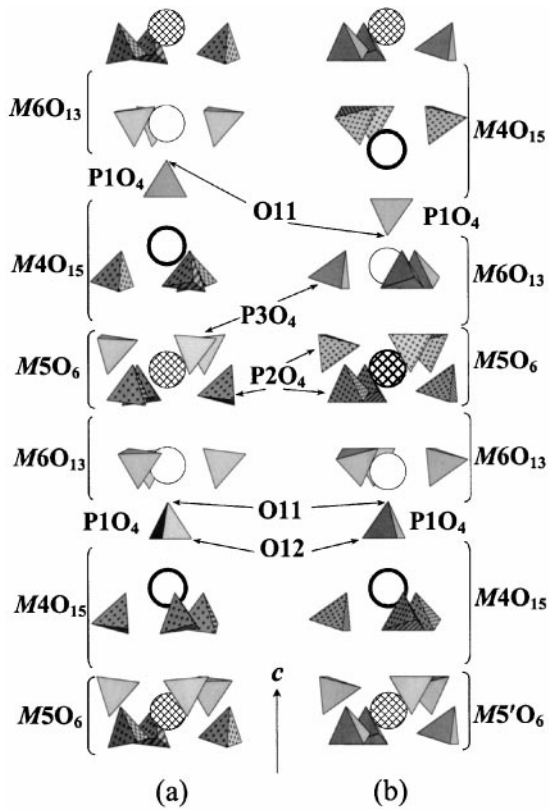

FIG. 4. Columns *A* with surrounding tetrahedra in (a) β-$Ca_3(PO_4)_2$ and (b) the ideal centrosymmetric β-$Ca_3(PO_4)_2$-like structure. Atom labels are the same as those in Fig. 2.

$a = 5.3901$ Å, $c = 19.785$ Å, and $Z = 3$) (37). Projections of the three structures viewed along the [110] and [001] directions are shown in Figs. 2 and 3. The structure of $Sr_3(PO_4)_2$ can be constructed from one type of layers, I (layers II shown in Figs. 2g and 3c are equivalent with layers I). Layer I contains one type of columns *B* (columns *A* shown in Fig. 2g are equivalent to columns *B*). The structures of $Sr_{9.1}Cu_{1.4}(PO_4)_7$ and β-$Ca_3(PO_4)_2$ (31, 32) can be constructed from two types of layers I and II. Layer I contains columns *B*, while layer II contains columns *A* and *B*. Layers I and columns *B* are very similar for the three structures (Figs. 2b, 2f, and 2h). The differences among the three structures are in layers II and columns *A*. The structure of $Sr_{9.1}Cu_{1.4}(PO_4)_7$ may be considered as the intermediate structure between β-$Ca_3(PO_4)_2$ and $Sr_3(PO_4)_2$. But the structure of $Sr_{9.1}Cu_{1.4}(PO_4)_7$ is topologically closer to the structure of β-$Ca_3(PO_4)_2$ because they are distinguished by different site occupancies (sites *M*4 and *M*6) and by different $P1O_4$ tetrahedra orientations (Figs. 2a and 2e). While the difference between $Sr_3(PO_4)_2$ and $Sr_{9.1}Cu_{1.4}(PO_4)_7$ involves elimination of tetrahedra from columns *A* in addition to different site occupancies and tetrahedra orientations (Figs. 2e and 2g).

The ideal centrosymmetric β-$Ca_3(PO_4)_2$-like structure without disordering is shown in Figs. 2c, 2d, and 4b. This structure can be described by space groups $R\bar{3}$ or $R\bar{3}m$ with the same cell dimensions as in β-$Ca_3(PO_4)_2$. But this ideal ordered structure does not take place in $Sr_{9.1}Cu_{1.4}(PO_4)_7$. In fact, $Sr_{9.1}Cu_{1.4}(PO_4)_7$ has the reduced *c* parameter by a factor of 2 in comparison with β-$Ca_3(PO_4)_2$ and many disordered elements in its crystal structure. In the $R\bar{3}m$ model of $Sr_{9.1}Cu_{1.4}(PO_4)_7$ the phosphorus atoms P1 lie in the center of symmetry that cannot be in a real structure. Displacement of the oxygen atoms O11 and copper atoms in the *M*4 sites from the threefold axis and disordering of strontium cations in the *M*3 site may indicate that the symmetry of the real structure deviates from trigonal, as was found for $Sr_9In(PO_4)_7$ (space group $P2/c$, $Z = 4$, $a = 18.3716(2)$ Å, $b = 10.66321(4)$ Å, $c = 18.0428(2)$ Å, and $\beta = 132.9260(5)^\circ$) with synchrotron XRD data (39). But XRD pattern of $Sr_{9.1}Cu_{1.4}(PO_4)_7$ showed no superstructure reflections and no splitting of reflections. In addition, studies of isotypic compounds, $Sr_{9.2}Co_{1.3}(PO_4)_7$ by single-crystal X-ray diffraction (36), $Sr_{9.3}Ni_{1.2}(PO_4)_7$ by neutron powder diffraction and electron microscopy (ED and HREM) (these data will be published elsewhere), and $Sr_{9+x}M_{1.5-x}(PO_4)_7$ (M = Mn, Fe, Co, Ni, and Cd) (13, 40) by X-ray powder diffraction, in combination with SHG data, have confirmed the $R\bar{3}m$ space group with $a \approx 10.6$ Å and $c \approx 19.7$ Å, partial occupation of the *M*4 sites, and disordering of $P1O_4^{3-}$ tetrahedra and strontium cations in the *M*3 site.

Some contradictions between the results of the crystal structure refinement and Mössbauer data for $Sr_9Fe_{1.5}(PO_4)_7$ were found (13). These contradictions were explained by the disordered character of the $Sr_9Fe_{1.5}(PO_4)_7$ structure and by the fact that Mössbauer spectroscopy gives information about local environments of iron cations, while XRD data give an average crystal structure. The same situation is observed for $Sr_{9.1}Cu_{1.4}(PO_4)_7$. Copper cations in $Sr_{9.1}Cu_{1.4}(PO_4)_7$ have a rather unusual oxygen surrounding. Copper cations occupy the trigonal-distorted octahedral *M*5 site and the large cavity *M*4. In the $M5O_6$ octahedron all six copper–oxygen distances are the same, which is not usual for the Jahn–Teller copper cation. Probably, distortions caused by the Jahn–Teller effect take place but it is not possible to detect by X-ray diffraction methods. Copper cations in the *M*4 site are displaced from the threefold axis because the distances between the threefold axis and oxygen environment are too large for copper cations (2.35–2.42 Å). A similar oxygen environment was observed in $Ca_9Cu_{1.5}(PO_4)_7$ (30). Unusual oxygen surrounding of copper cations is a possible reason for the instability of $Sr_{9.1}Cu_{1.4}(PO_4)_7$ in comparison with other isostructural compounds $Sr_{9.2}Co_{1.3}(PO_4)_7$ (36), $Sr_9Fe_{1.5}(PO_4)_7$ (13), and $Sr_{9+x}M_{1.5-x}(PO_4)_7$ (M = Mn, Ni, and Cd) (40).

Polyhedra for the ideal *M*3 sites (that is, in site $9e$ ($\frac{1}{2}$, $\frac{1}{2}$, 0)) without O11 atoms are shown in Fig. 5. These polyhedra have four quadrilateral faces O21–O21a–O22–O22a and

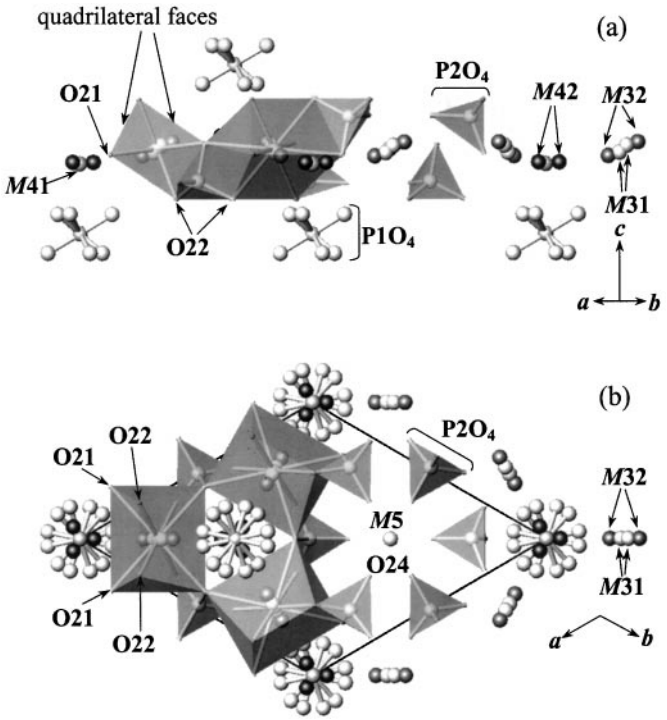

FIG. 5. Fragments of the crystal structure of $Sr_{9.1}Cu_{1.4}(PO_4)_7$ viewed along (a) the [110] and (b) [001] directions. Polyhedra for the ideal *M*3 site are emphasized.

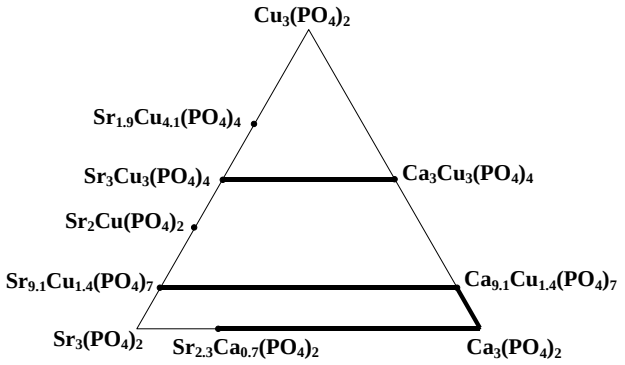

FIG. 6. Phases and solid solution regions known in the system $Ca_3(PO_4)_2$–$Sr_3(PO_4)_2$–$Cu_3(PO_4)_2$.

can be considered as incomplete without O11 atoms. But distances $M3$–O11 = 3.11 Å are large, which likely results in the displacement of strontium cations toward one of the O11 atoms. The presence of cations in the $M4$ sites results in the oxygen atoms around the P1 site not being located on the threefold axis. Otherwise, the $M4$–O distances would become very short. This is a possible reason for the $P1O_4$ tetrahedra disordering.

The compounds $Sr_{9.1}Cu_{1.4}(PO_4)_7$ and β-$Ca_3(PO_4)_2$ are structurally related. In its turn, solid solutions $Ca_{10.5-x}Cu_x(PO_4)_7$ ($0 \le x \le 1.5$) with the β-$Ca_3(PO_4)_2$ structure exist (30, 41, 42). Thus, formation of solid solutions $Sr_{9.1-x}Ca_xCu_{1.4}(PO_4)_7$ ($0 \le x \le 9.1$) might be proposed, which was confirmed (see Table 8). The specimens with $x = 9.1$ and 6.825 were indexed in space group $R3c$ (as β-$Ca_3(PO_4)_2$) because of the presence of weak reflections with odd indexes l, while only reflections with even indexes l were observed on XRD patterns of the specimens with $x = 4.55$, 2.1, and 0.7, which make it possible to reduce the c parameter by a factor of 2 (Table 8) as for $Sr_{9.1}Cu_{1.4}(PO_4)_7$. In the system $Ca_{3-x}Sr_x(PO_4)_2$ solid solutions with the β-$Ca_3(PO_4)_2$ structure are formed at $0 \le x \le 2.3$ (1, 41, 43). Thus, solid solutions in the region β-$Ca_3(PO_4)_2$–$Ca_{9.1}Cu_{1.4}(PO_4)_7$–$Sr_{9.1}Cu_{1.4}(PO_4)_7$–$Sr_{2.3}Ca_{0.7}(PO_4)_2$ may exist (Fig. 6).

ACKNOWLEDGMENTS

This work was supported by the Russian Foundation for Basic Research (Grants 00-03-32660, 01-03-06122, and 01-03-06123). Authors thank Dr. S.Yu. Stefanovich (Moscow State University) for SHG study.

REFERENCES

1. J. F. Sarver, M. V. Hoffman, and F. A. Hummel, *J. Electrochem. Soc.* **108,** 1103 (1961).
2. J. R. Looney and J. J. Brown, *J. Electrochem. Soc.* **118,** 470 (1971).
3. H. Koelmans and A. P. M. Cox, *J. Electrochem. Soc.* **104,** 442 (1957).
4. H. Donker, W. M. A. Smit, and G. Blasse, *J. Electrochem. Soc.* **136,** 3130 (1989).
5. V. Pelova, K. Kynev, and G. Gochev, *J. Mater. Sci. Lett.* **14,** 330 (1995).
6. A. Hemon and G. Courbion, *J. Solid State Chem.* **85,** 164 (1990).
7. B. Elbali, A. Boukhari, J. Aride, and F. Abraham, *J. Solid State Chem.* **104,** 453 (1993), doi:10.1006/jssc.1993.1180.
8. B. Elbali and A. Boukhari, *Acta Crystallogr. C* **49,** 1131 (1993).
9. B. Elbali, A. Boukhari, E. M. Holt, and J. Aride, *J. Crystallogr. Spectosc. Res.* **23,** 1001 (1993).
10. A. A. Belik, B. I. Lazoryak, T. P. Terekhina, and S. N. Polyakov, *Russ. J. Inorg. Chem.* **46**(9), 1312 (2001).
11. B. El-Bali, A. Boukhari, R. Glaum, M. Gerk, and K. Maass, *Z. Anorg. Allg. Chem.* **626,** 2557 (2000).
12. H. Effenberger, *J. Solid State Chem.* **142,** 6 (1999), doi:10.1006/jssc.1998.7953.
13. A. A. Belik, B. I. Lazoryak, K. V. Pokholok, T. P.Terekhina, I. A. Leonidov, E. B. Mitberg, V. V. Karelina, and D. G. Kellerman, *J. Solid State Chem.*, doi:10.1006/jssc.2001.9363.
14. A. Moqine, A. Boukhari, and J. Darriet, *J. Solid State Chem.* **107,** 362 (1993), doi:10.1006/jssc.1993.1359.
15. B. El-Bali, M. Bolte, A. Boukhari, J. Aride, and M. Taibe, *Acta Crystallogr. C* **55,** 701 (1999).
16. K. M. S. Etheredge and S.-J. Hwu, *Inorg. Chem.* **35,** 1474 (1996).
17. F. Lucas, G. Wallez, S. Jaulmes, A. Elfakir, and M. Quarton, *Acta Crystallogr. C* **53,** 1741 (1997).
18. R. Vogt and Hk. Muller-Buschbaum, *Z. Anorg. Allg. Chem.* **591,** 167 (1990).
19. M. von Postel and Hk. Muller-Buschbaum, *Z. Anorg. Allg. Chem.* **615,** 97 (1992).
20. D. Osterloh and Hk. Muller-Buschbaum, *Z. Anorg. Allg. Chem.* **620,** 651 (1994).
21. S. Eymond, A. Durif, and C. Martin, *C. R. S. Acad. Sci. Ser. C* **268,** 1694 (1969).
22. A. Boukhari, A. Moqine, and S. Flandrois, *Mater. Res. Bull.* **21,** 395 (1986).
23. M. Drillon, M. Belaiche, P. Legoll, J. Aride, A. Boukhari, and A. Moqine, *J. Magn. Magn. Mater.* **128,** 83 (1993).
24. J. B. Anderson, E. Kostiner, and F. A. Ruszala, *J. Solid State Chem.* **39,** 29 (1981).
25. H. M. Rietveld, *Acta Crystallogr.* **22,** 151 (1967).
26. F. Izumi and T. Ikeda, *Mater. Sci. Forum* **321–324,** 198 (2000).
27. H. Toraya, *J. Appl. Crystallogr.* **23,** 485 (1990).
28. "International Tables for Crystallography," Vol. C, pp. 500–503. Kluwer, Dordrecht, 1992.
29. P. E. Warner, L. Eriksson, and M. Westdahl, *J. Appl. Crystallogr.* **18,** 367 (1985).
30. A. A. Belik, O. V. Yanov, and B. I. Lazoryak, *Mater. Res. Bull.* **36,** 1863 (2001).
31. B. Dickens, L. W. Schroeder, and W. E. Brown, *J. Solid State Chem.* **10,** 232 (1974).
32. B. I. Lazoryak, *Rus. Chem. Rev.* **65,** 287 (1996).
33. B. I. Lazoryak, V. A. Morozov, A. A. Belik, S. S. Khasanov, and V. Sh. Shekhtman, *J. Solid State Chem.* **122,** 15 (1996), doi:10.1006/jssc.1996.0074.
34. A. A. Belik, V. A. Morozov, S. S. Khasanov, and B. I. Lazoryak, *Mater. Res. Bull.* **34,** 883 (1999).
35. B. I. Lazoryak, N. Khan, V. A. Morozov, A. A. Belik, and S. S. Khasanov, *J. Solid State Chem.* **145,** 345 (1999), doi:10.1006/jssc.1999.8294.
36. A. A. Belik and B. I. Lazoryak, unpublished results.
37. K. Sugujama and M. Tokonami, *Mineral J.* **15,** 141 (1990).

38. D. Osterloh and Hk. Muller-Buschbaum, *J. Alloys Compd.* **206,** 155 (1994).
39. A. A. Belik, F. Izumi, T. Ikeda, M. Okui, A. P. Malakho, and B. I. Lazoryak, *J. Solid State Chem.*, submitted.
40. A. A. Belik, A. P. Malakho, B. I. Lazoryak, and S. S. Khasanov, *J. Solid State Chem.*, submitted.
41. A. G. Nord, *N. Jb. Miner. Mh.* **11,** 489 (1983).
42. A. Benarafa, M. Kacimi, G. Coudurier, and M. Ziyad, *J. Appl. Catal. A* **196,** 25 (2000).
43. A. Bigi, E. Foresti, M. Gandolfi, M. Gazzano, and N. Roveri, *J. Inorg. Biochem.* **66,** 259 (1997).